Chaotic Modeling and Simulation (CMSIM) 1: 117-131 , 2013

Utilisation of the Perturbation Theory without Presuppositions. A Repeating Equation for Azimouthal Velocities into Cylindrical and Magnetized Plasma

C. L. Xaplanteris[1,2], E. D. Filippaki[1], I. S. Mistakidis[2] and L. C. Xaplanteris[3]

(1) Plasma Physics Laboratory, IMS, NCSR "Demokritos", Athens , Greece
(2) Hellenic Military Academy , Vari Attica , Greece .
(3) School of Physics, National and Kapodistrian University of Athens , Greece .
(E-mail: cxaplanteris@yahoo.com)

Abstract: As the understanding of the chaotic state increases, it becomes clearer that the definition and the theoretical elaboration of the chaos is not a simple hypothesis. In addition, it is a commonplace fact that the mathematical representation of the chaos theory on the whole is very difficult to be given. This means that there is not any mathematical equation capable of describing and solving a nonlinear and chaotic problem. So, as every case is unique, our work has to contribute to the chaotic topic both mathematically and experimentally. Magnetized argon plasma is produced into a metallic cylinder. A coaxial antenna is used for the r-f energy importation and the plasma maintenance consequently. This device has a complete cylindrical symmetry and the mathematic elaboration in the cylindrical system is carried out. An attempt to show a repeating relation for ion velocities of magnitude of every order is presented as our new work. In addition, it is well known that the perturbation theory can be used to extend the linear theory of plasma waves into the nonlinear regime and, thus, give an explanation of many nonlinear phenomena. This nonlinear perturbation theory of small amplitude plasma waves and their interactions is well developed; on the contrary, the perturbation theory of large-amplitude plasma waves is still being developed. In the present paper, a generalization of the perturbation theory is attempted with the division of the perturbed magnitude and the use of the repeating estimation. Computational results and experimental findings are in a very satisfactory accordance.
Keywords: Chaos theory, Nonlinear problem, Cylindrical system, r-f plasma production, Repeating relation, Perturbation theory, Loop on the repeating relation.

1. Introduction

The stability and instability of the plasmatic state was an old problem for researchers during the last decades. Especially, in the early 60's many plasma

Received: 10 December 2012 / Accepted: 22 January 2013

ISSN 2241-0503

instabilities have been observed taking wavy forms into the plasma [1-4]. These waves absorb the plasma energy, then the plasma temperature is consequently reduced and the removal of the thermonuclear fusion conditions is resulted. So, the wavy instabilities are considered to be a serious obstacle to the nuclear fusion process and their study has been carried out constantly and in detail during the last decades [5,6]. Many special books constitute the Plasma Physics Literacy [7-10], list and study all the waves from the low frequency region [1-6] to the high frequency one [11]. In the Plasma Laboratory of the Center "Demokritos" an adequate amount of experience has been gained, especially on the low frequency electrostatic waves [12-14] and their effect on the plasma conductivity [13]. The chaotic behavior of the plasma waves has been studied as well [15,16]. It is well known that the plasma can easily pass from a steady state into a chaotic one, which was repeatedly published in our previous papers [17,18]. In the present work an attempt takes place to compare the experimental data with the computation results, and so, our theory may be confirmed. A mathematic relation, which connects the different order velocities, was found and may be used as a repeating relation showing the chaotic behavior of the plasma. The relation is valid under the condition that the perturbed qualities are small in comparison with the unperturbed one [8-10]. In the present work a calculative trial using the relation as a repeating one may bring it into the function conditions and the perturbed theory can be therefore extended. Although the experimental results are in a satisfactory agreement with the calculation, the subject remains open as a chaotic state one and requires further study. In the next research of ours, the influence of the initial conditions on the computational results is planed to be studied.

A brief description of the experimental devices is given in Sec.2, since the experimental results are presented in the following Sec.3. In Sec. 4 a full mathematical elaboration and the computational results are curried out. The confirmation between theory and experiment and conclusions are included in Sec. 5. A more detailed mathematical elaboration is provided in the Appendix at the end of the paper.

2. Description of the Experimental Set-Up

It is well known that the predominant direction of the external magnetic field $\vec{B}$ in the Q-machine is well matched with the cylindrical geometry of the device, when the cylinder axis and magnetic field coincide. As our experience on the magnetized argon plasma is concentrated on full cylindrical symmetry, the same geometry is used at the present study as well, since the low frequencies of plasma waves are persistent [1-4, 12-14]. A cylindrical cavity made of steady steel is located with its' axis along the external magnetic field B. The cavity is $60cm$ long with $6cm$ internal diameter and, in the center of the first disk-like base, the $25cm$ rf power antenna is mounted; in the other disk-like base a $25cm$ external driving wave antenna is mounted as well, which enables us to affect and control the plasma waves. Electrostatic Langmuir probes were fixed to move radially, azimouthally and axially with the ability to detect the plasma waves that appear and measure their physical quantities (wave frequency, wave amplitude, plasma temperature, plasma density, plasma potential e.t.c.). Furthermore, a disk-probe was fixed to move radially and around its' axis, which allows, apart from the above quantities, the measuring of the azimouthal electron drift current. In Fig.1 (a) the plasma column cut is shown, whereas an extensive drawing of the cavity's position into the magnetic field is presented in Fig.1 (b).

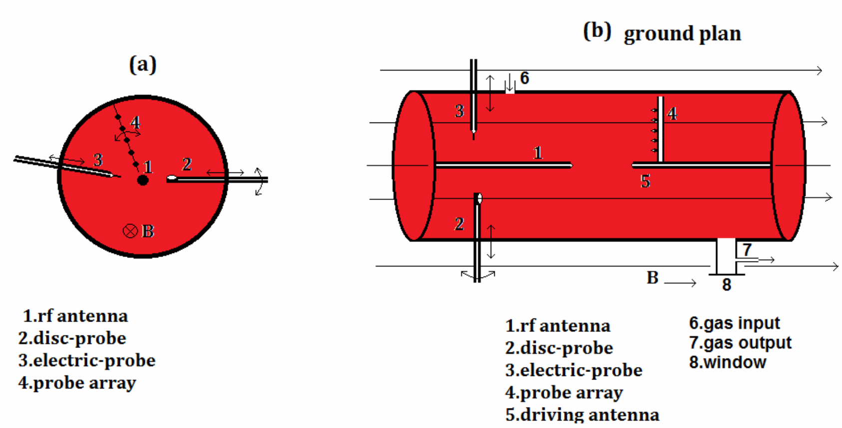

Fig.1 (a), the plasma column is shown. Fig.1 (b), the cavity's placing into the magnetic field is presented (ground plan).

The argon entrance, its' outlet to the pump and a suitable window are placed on the curved surface of the cylinder, as they are represented at the Fig.1 (b).

3. Experimental Data

The existence of the electrical waves into the argon plasma is confirmed once more. These low frequency waves are divided into three frequency regions with a quasi-same behavior in many instances. An extensive study of these waves was carried out at the Plasma Laboratory of NCSR ''Demokritos'' previously, and two of them were absolutely identified [12, 14]. A stable dependence of the gas pressure on the waves has been presented and measured again. This influence consists of the simultaneous decrease of the waves' amplitude and frequency as the gas pressure increases. Figures 2 and 3 give a middle frequency region wave indicatively with its' spectrum of frequencies where the upper harmonics appear; the first with a high value of the gas pressure and the second with a low one.

The plasma is lit into an wide space of the external plasma parameters (gas pressure p, magnetic field B and rf field absorbed power P) and results in a wide region of plasma quantities as well; these quantities include the plasma temperature T, the plasma density n, the plasma potential Φ, and all the wave parameters. Table 1 shows some typical values of the plasma parameters.

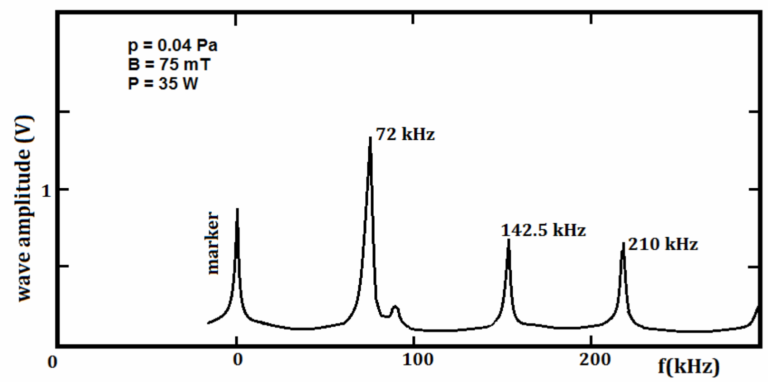

Fig. 2. A typical wave spectrum in the middle frequency region with high gas pressure.

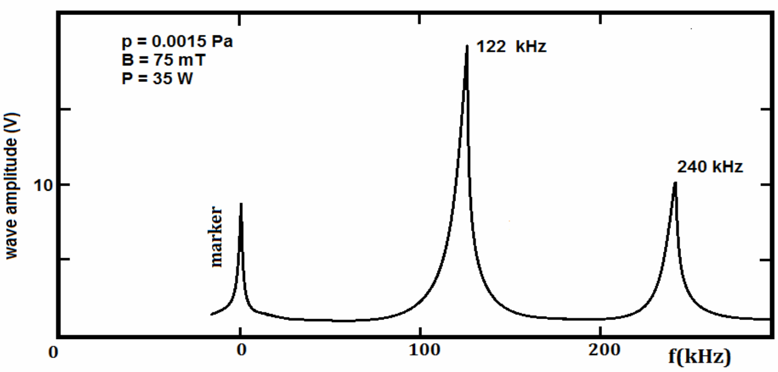

Fig. 3. A typical wave spectrum in the middle frequency region again with low gas pressure.

Table 1 The plasma parameters ranging values

Parameters	Minimum value	Maximum value
Argon pressure p	$0.001\,Pa$	$0.1\,Pa$
Argon number density, n_g	$2\times10^{15}\,m^{-3}$	$2\times10^{17}\,m^{-3}$
Magnetic field intensity, B	$10\,mT$	$200\,mT$
Microwaves' power, P	$20\,Watt$	$120\,Watt$
Frequency of the rf power (standard value)	$2.45\,GHz$	
Electron density, n_0	$2\times10^{15}\,m^{-3}$	$4.6\times10^{15}\,m^{-3}$
Electron temperature, T_e	$1.5\,eV$	$10\,eV$
Ion temperature, T_i	$0.025\,eV$	$0.048\,eV$
Ionization rate	0.1%	90%
Electron drift velocity, u_e	$1\times10^{4}\,{}^{m}\!/_{s}$	$1.7\times10^{4}\,{}^{m}\!/_{s}$
Electron-neutral collision frequency, ν_e	$1.2\times10^{7}\,s^{-1}$	$3\times10^{9}\,s^{-1}$

The experimental part of the present paper consists of the following steps:

i) By using the radial moving probe, the plasma potential $\Phi(r)$ is measured along the cylinder radius and then, from the relation $\varepsilon = -\dfrac{\Delta\Phi}{\Delta r}$ the plasma electric field ε is calculated. Figure 4 is shows the radial potential and radial electric field along the cylinder radius.

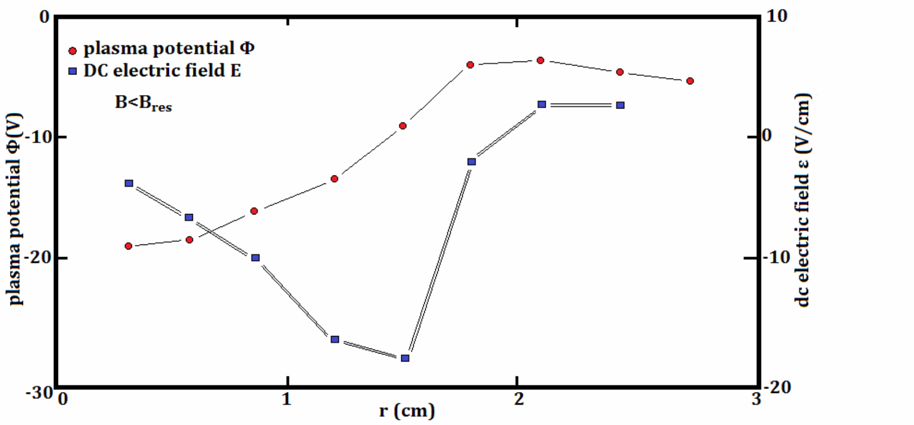

Fig.4 shows the plasma potential $\Phi(r)$ and the electric field ε along the cylinder radius.

It must be noted that the electric field ε remains nearly constant in the middle of the radius, where the wave rises and its' amplitude constantly increases [6, 12-14]. The measurement has been done by $B \prec B_0$.

ii) The perturbed electric field E must be measured, consequently. This measurement may be a result of the wave amplitude as it appears along the cylinder radius. Figure 5 is shows the wave amplitude (in Volts) and the perturbed field E correspondingly. The measurement was repeated for values of the magnetic field B , under and above the upper cyclotron resonance B_{res} .

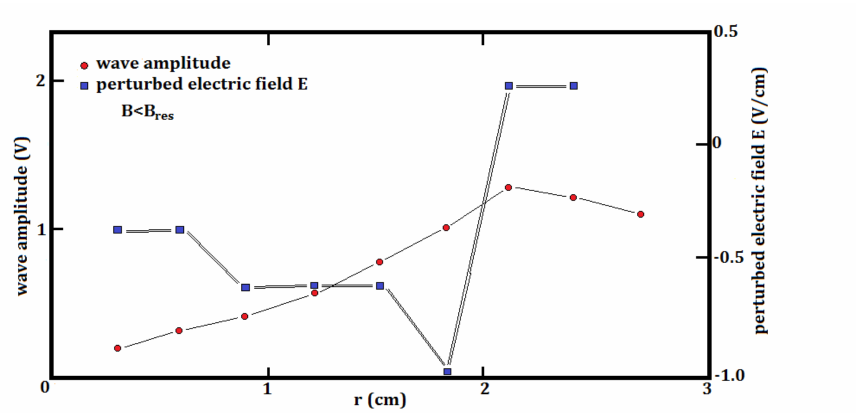

Fig. 5 shows the wave amplitude and the perturbed electric field E along the cylinder radius.

iii) The measurement of the azimouthal electron drift velocity u_e is the next step. This is obtained by using the disk probe as it moves around its' axis. Figure 6 indicates the method of the measurement of the azimouthal electron current I_θ , which requires two simple movements: the orientation of the probe surface perpendicularly to the electron drift course, and after, in the opposite direction of the electrons' motion.

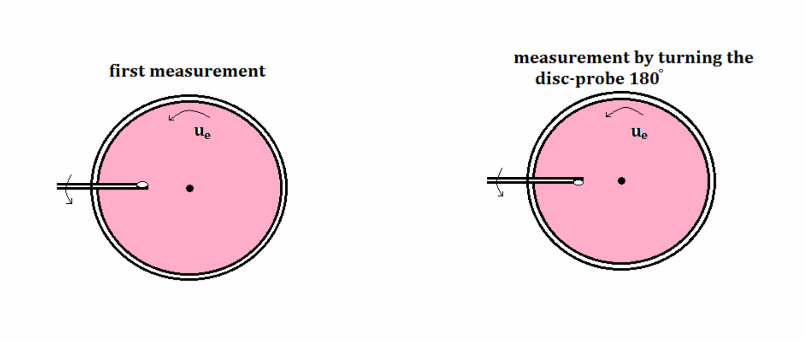

Fig. 6, the electron drift current measurement

The next relations $I_1 = I_\theta + I_{th}$ and $I_2 = -I_\theta + I_{th}$ are valid and result in the relation below,

$$I_\theta = \frac{I_1 - I_2}{2}$$

Taking into consideration that the relation $I_\theta = e.n_e.u_e.$A is valid (with A the probe surface area), the azimouthal electron drift can be found. Measurements and estimations are listed in Table 2, **s**ince the electron drift velocity u_e and the perturbed velocity υ are presented in Fig. 7, as well.

Table 2 The azimouthal electron drift current and the drift velocity along a cylinder radius

Radius r (cm)	drift current I_e (μA)	plasma density n_e ($x\mathbf{10^{15}}\, m^{-3}$)	drift velocity u_e ($x10^3\, m/s$)	E/ε	perturbed velocity υ_θ (m/s)
0.3	20	6.0	4.43	−0.1	−443
0.6	26	6.2	5.57	−0.05	−278
0.9	30	6.5	6.17	−0.067	−413
1.2	37	7.0	7.02	0.04	281
1.5	42	6.8	8.20	0.037	303
1.8	46	6.2	9.85	0.25	2462
2.1	35	5.9	7.92	0.1	792
2.4	25	5.6	5.93	0.1	593
2.7	16	5.5	3.86		

iv) The perturbed velocity υ_θ is impossible to be found directly by an experimental measuring, but it can be estimated from the relation $\upsilon_\theta = \frac{E}{\varepsilon} u_\theta$, as the quantities ε, E and u_θ have been measured above. The results for the υ are given again in Table 2.

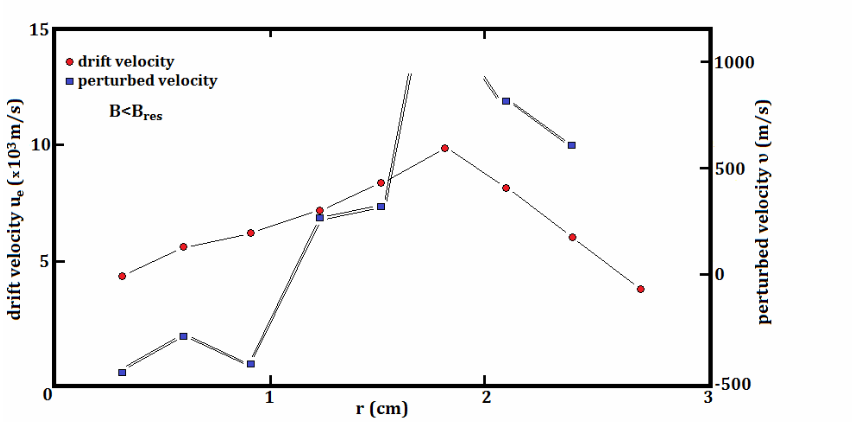

Fig.7. The drift velocity u_e and the perturbed velocity υ are presented

4. Mathematical Elaboration - Computational Results

Perturbed velocities' study

In the Appendix it is proved that the drift and perturbed velocities are related to the electrical fields with the Eq. (A. 9),

$$\upsilon_r = \frac{E}{\varepsilon} u_r \quad \text{and} \quad \upsilon_\theta = \frac{E}{\varepsilon} u_\theta \qquad \text{(A. 9)}$$

A. When the perturbed electric field E is very small, then the relations $\upsilon_r \prec u_r$ and $\upsilon_\theta \prec u_\theta$ are valid.

B. If the relation $\upsilon \approx u$ is valid, the electric fields must have the same behavior as $E \approx \varepsilon$. This means that the wave amplitude undergoes some big changes along the cylinder radius.

With the replacement of the quantity Π , the Eqs (A. 7) are written:

$$\upsilon_\theta = \frac{E}{B} \cdot \frac{\omega_c^2}{\omega_c^2 + \left[j(ku - \omega) + \nu \right]^2} \qquad \text{and} \qquad \upsilon_r == \frac{E}{B} \cdot \frac{\omega_c \left[j(ku - \nu) + \nu \right]}{\omega_c^2 + \left[j(ku - \omega) + \nu \right]^2}$$

(1)

The azimouthal perturbed velocity υ_θ is of the most interest: by taking $\Pi^2 = \nu^2 - (ku - \omega)^2 + j2\nu(ku - \omega)$ and limiting the real part only, the first of Eqs (1) is rewritten as following,

$$\upsilon = \frac{E}{B} \cdot \frac{\omega_c^2}{\omega_c^2 + \nu^2 - (ku - \omega)^2} \qquad (2)$$

with $\upsilon_\theta = \upsilon$ for simplicity; this may be used as the repeating relation.

It must be reminded that the Eq.(A. 9) was produced with the presupposition that the relation $\upsilon \prec\prec u$ is valid. This consists a necessary condition for the linearization of Eq. (A. 1) (perturbation theory).

Now, if we seek a solution for $\upsilon \approx u$, approximately, by separating the perturbed velocity υ into small parts $\upsilon_1, \upsilon_2, \upsilon_3, ...\upsilon_i$ with $i = 10,100,1000,....$ and every part $\upsilon_i \prec\prec \upsilon$, the perturbation theory condition is satisfied.

Taking $u = u_0$ and $\upsilon = \upsilon_1 \prec \frac{\upsilon}{10}$, the Eq. (2) is written,

$$\upsilon_1 = \frac{E}{B} \cdot \frac{\omega_c^2}{\omega_c^2 + \nu^2 - (ku_0 - \omega)^2} \qquad (3)$$

With the addition $u_1 = u_0 + \upsilon_1$, the above equation gives the term υ_2,

$$\upsilon_2 = \frac{E}{B} \cdot \frac{\omega_c^2}{\omega_c^2 + \nu^2 - (ku_1 - \omega)^2}$$

If it is taken $u_2 = u_1 + \upsilon_2$, the Eq. (2) gives the term υ_3,

And so on, with $u_{i+1} = u_i + \upsilon_{i+1}$ the repeating relation,

$$\upsilon_{i+1} = \frac{E}{B} \cdot \frac{\omega_c^2}{\omega_c^2 + \nu^2 - (ku_i - \omega)^2} \qquad (4)$$

is obtained.

<u>Repeating equation study</u>

It is evident that the minimum value of the term $(ku_i - \omega)^2$ is zero, and then the denominator in the Eq. (4) takes the maximum value. Then, we conclude that, at the value $u_i = \dfrac{\omega}{k}$, the υ_{i+1} has the minimum value, $\upsilon_{i+1} = \dfrac{E}{B}\dfrac{\omega_c^2}{\omega_c^2 + \nu^2}$, which is the same as if the quality $\Pi = j(ku - \omega) + \nu \cong \nu$, is taken.

Another significant result is obtained if the relations $u_1 = u_0 + \upsilon_1$, $u_2 = u_1 + \upsilon_2$, $u_3 = u_2 + \upsilon_3$, ...$u_i = u_{i-1} + \upsilon_i$, are added by parts, when the relation $u_i = u_0 + \upsilon_1 + \upsilon_2 + \upsilon_3 + ... + \upsilon_i$ or

$$u_i = u_0 + \upsilon \qquad (5)$$

is obtained

with $\upsilon = \upsilon_1 + \upsilon_2 + \upsilon_3 + ... + \upsilon_i$ the whole-total large perturbed velocity.

The relation $u_i = u_0 + \upsilon$ must be confirmed experimentally.

Computational results

The experiment leads to the following calculations;

$$\frac{E}{B} \cong \frac{100V.m^{-1}}{70.mT} \qquad \Rightarrow \underline{\frac{E}{B} \cong 1430\frac{m}{s}},$$

$$\omega_c^2 = \left(\frac{e.B}{m_e}\right)^2 = \left(\frac{1{,}6.10^{-19}.7.10^{-2}}{9{,}1.10^{-31}}\right)^2, \qquad \underline{\Rightarrow \omega_c^2 \cong 1{,}5.10^{20}\, s^{-2}}$$

$$\underline{\nu^2 \cong 10^{19}\, s^{-2}}$$

When it is taken $ku_0 - \omega = 0$, then $u_0 = \omega/k = \omega.R/l \Rightarrow u_0 = \omega.R/l$.

Taking $\omega = 2\pi.f = 2\pi.7.10^4\, s^{-1} \quad \Rightarrow \omega = 1{,}4.\pi.10^5\, s^{-1}$, $l = 1$ and $R = 2.10^{-2}\, m$ then

$$u_0 = 1{,}4.\pi.10^5.2.10^{-2}\, m/s \qquad \underline{\Rightarrow u_0 \cong 0{,}88.10^4\, m/s}$$

In the above case the perturbed velocity υ_1 is minimized at the value, (see eq. 3) ,

$$\upsilon_1 = 1430.\frac{10^{20}}{10^{20}+10^{19}} {}^{m}\!/\!{}_{s} \qquad \Rightarrow \upsilon_1 \cong 1300 {}^{m}\!/\!{}_{s}$$

On the other hand, the relation $\upsilon = {}^{E}\!/\!{}_{\varepsilon}\, u$ gives,

$$\upsilon = {}^{2V.cm^{-1}}\!/\!{}_{20V.cm^{-1}} .u \qquad \Rightarrow \upsilon = 880 {}^{m}\!/\!{}_{s}$$

Now, with $u_1 = u_0 + \upsilon_1 = (8800+880) {}^{m}\!/\!{}_{s}$ $\Rightarrow u_1 = 9680 {}^{m}\!/\!{}_{s}$, the perturbed υ_2 from the repeating equation below can be calculated,

$$\upsilon_2 = \frac{E}{B}.\frac{\omega_c^2}{\omega_c^2 + \nu^2 - (ku_1 - \omega)^2}$$

or

$$\upsilon_2 = 1430.\frac{1,5.10^{10}}{16.10^9 - (5.0,968 - 4,4)^2}$$

or

$$\upsilon_2 = 1340,62499998377843750019$$

Now it is taken, $u_2 = u_1 + \upsilon_2$, $\Rightarrow u_2 = 9680 + 1340,62499998377843750019$ $\Rightarrow u_2 = 11020,62499998377843750019$, and so on.

5. Explanation- Conclusions

The existence of the low frequency waves into the argon magnetized plasma was observed in our early experiments at the Plasma Laboratory of Demokritos. A satisfactory explanation about it was given as well [12,14]. In previous publication the possibility for development of the low frequency waves has been presented. Two kinds of these waves have been identified already [12, 14]. The cylindrical symmetry of the plasma column gives them azimouthal propagation, whereas the boundaries cause for standing waves formation. By using the perturbation theory on the two fluids model, the relation,

$$\upsilon = \frac{E}{B}.\frac{\omega_c^2}{\omega_c^2 + \nu^2 - (ku - \omega)^2}$$

is obtained under the conditions $\upsilon \prec\prec u$.

The validity of the above equation is attempted to be proved with the present experiment. So, the value of the perturbed velocity υ was found at first experimentally and then by estimation from the above equation. The direct measurement of the perturbed velocity υ is impossible to be carried out as it is added on the drift velocity u , resulting in the inability to be distinguished from it. For this reason, the relation $\upsilon = E/_{\varepsilon} .u$ was used, which requires the measurement of the quantities E , ε and u . As Figs 4 and 5 show, the electric fields E and ε are maximized in the middle of the radius, where the wave is developed, and the ratio $E/_{\varepsilon}$ is very close to the perturbation theory condition. Furthermore, from Table 2 the values of the drift electron velocity are taken. Figure 7 gives the measured values of the perturbed velocity υ . Afterwards, the calculated values from the repeating equation are taken. Despite the inevitable inclinations of the measurements, the two results are satisfactory close, and may have the certainty that the suggested calculation method is right. Another significant observation is that, because of the use of the equation as a repeating one, the values of the perturbed velocity are slightly affected from the drift velocity enlargement. On the contrary, the drift velocity enlargement strengthens the function condition $\upsilon \prec\prec u$.

Appendix

The momentum equation on the two fluids theory based on a non-local slab is written as,

$$N_\alpha m_\alpha [\ \frac{\partial}{\partial t} + \vec{V}_\alpha.\vec{\nabla})\ ]\vec{V}_\alpha = N_\alpha q_\alpha (\vec{\varepsilon} + \vec{E}) + N_\alpha q_\alpha \frac{\vec{V}_\alpha x\vec{B}}{c} - N_\alpha m_\alpha \nu \vec{V}_\alpha - \vec{\nabla} p$$

where the indicator α is given for both kinds of the charged particles, electrons and ions. In the following elaboration, the α is omitted for simplicity and the momentum equation for either electrons and ions becomes,

$$N\ m\ [\ \frac{\partial}{\partial t} + \vec{V}.\vec{\nabla})\ ]\vec{V} = Nq(\vec{\varepsilon} + \vec{E}) + Nq\frac{\vec{V}x\vec{B}}{c} - Nm\ \nu\vec{V} - \vec{\nabla} p \qquad \text{(A.1)}$$

where $N = n_0 + n(\vec{r},t), \vec{E}_{tot} = \vec{\varepsilon} + \vec{E}(\vec{r},t)$, and $\vec{V} = \vec{u}_0 + \vec{\upsilon}(\vec{r},t)$,

and $n(\vec{r},t), \vec{E}(\vec{r},t)$, and $\vec{\upsilon}(\vec{r},t)$, the perturbed qualities with harmonic influence $\propto e^{j(\vec{k}\vec{r} - \omega t)}$.

When no perturbation exists, the drift velocity u_0 , is obtained;

$$0 = n_0 q\vec{\varepsilon} + n_0 q \frac{\vec{u}_0 x\vec{B}}{c} - n_0 m \nu \vec{u}_0 \qquad \text{(A. 2)}$$

With the separation on the $\vec{r}$ and θ axis the drift components are given,

$$u_\theta = \frac{q\varepsilon}{m}.\frac{\omega_c}{\omega_c^2 + \nu^2} \qquad \text{and} \qquad u_r = \frac{q\varepsilon}{m}.\frac{\nu}{\omega_c^2 + \nu^2} \qquad \text{(A. 3)}$$

(drift velocities are represented by the 0-order equation).

i) If the perturbation is taken into account, eq.(A. 1) gives,

α)

$$n_0 \frac{\partial}{\partial t} + n_0 \vec{u}_0 \vec{\nabla}\vec{\upsilon} = n_0 \frac{q\vec{E}}{m} + n\frac{q\vec{\varepsilon}}{m} + nq\frac{\vec{u}_0 x\vec{B}}{mc} + n_0 q \frac{\vec{\upsilon} x\vec{B}}{mc} - n\nu\vec{u}_0 - n_0 \nu\vec{\upsilon} \qquad \text{(A. 4)}$$

(the 1st order equation)

β) $$n_0 \vec{\upsilon}.\vec{\nabla}\vec{\upsilon} + n\frac{\partial \vec{\upsilon}}{\partial t} + n\vec{u}_0.\vec{\nabla}\vec{\upsilon} = \frac{nq\vec{E}}{m} + nq\frac{\vec{\upsilon} x\vec{B}}{mc} - n\nu\vec{\upsilon} - \frac{\vec{\nabla}p}{m} \qquad \text{(A. 5)}$$

(the 2vd order equation)

γ) And finally,

$$n\vec{\upsilon}.\vec{\nabla}\vec{\upsilon} \cong 0 \qquad \text{(A. 6)}$$

(the 3rd order equation).

_ From the equilibrium state (zero order equation), the drift velocity components are easily obtained,

$$u_\theta = \frac{q\varepsilon}{m}.\frac{\omega_c}{\omega_c^2 + \nu^2} = \frac{\varepsilon}{B}.\frac{\omega_c^2}{\omega_c^2 + \nu^2} \qquad \text{and} \qquad u_r = \frac{q\varepsilon}{m}.\frac{\nu}{\omega_c^2 + \nu^2} = \frac{\varepsilon}{B}.\frac{\omega_c \nu}{\omega_c^2 + \nu^2}$$

_ From the first order equation, the perturbent velocity components may be given as,

$$\upsilon_\theta = \frac{qE}{m}.\frac{\omega_c}{\omega_c^2 + \Pi^2} = \frac{E}{B}.\frac{\omega_c^2}{\omega_c^2 + \Pi^2} \qquad \text{and}$$

$$\upsilon_r = \frac{qE}{m}.\frac{\Pi}{\omega_c^2 + \Pi^2} = \frac{E}{B}.\frac{\omega_c \Pi}{\omega_c^2 + \Pi^2} \qquad \text{(A. 7)}$$

with , $\Pi = j(ku - \omega) + \nu$

A combination of drift and perturbed velocities components gives,

$$\upsilon_\theta = \frac{E}{\varepsilon}\frac{\omega_c^2+\nu^2}{\omega_c^2+\Pi^2}.u_\theta \qquad \text{and} \qquad \upsilon_r = \frac{E}{\varepsilon}\frac{\Pi}{\nu}\frac{\omega_c^2+\nu^2}{\omega_c^2+\Pi^2}.u_r$$

(A. 8)

If it is considered that $ku-\omega \prec\prec \nu$, then it is taken $\Pi \cong \nu$ and the perturbed velocity components (eq.A. 7) become,

$$\upsilon_\theta = \frac{E}{B}.\frac{\omega_c^2}{\omega_c^2+\nu^2} \qquad \text{and} \qquad \upsilon_r = \frac{E}{B}.\frac{\omega_c\nu}{\omega_c^2+\nu^2}$$

as the drift velocity components by replacing the dc electric field ε with the perturbed one E.

If $ku-\omega \prec\prec \nu$, then $\Pi \cong \nu$ is taken likewise and from Eqs (A. 8) the below relations (A. 9) are obtained,

$$\upsilon_r = \frac{E}{\varepsilon}u_r \quad \text{and} \quad \upsilon_\theta = \frac{E}{\varepsilon}u_\theta \qquad \text{(A. 9)}$$

References

1. N.D'Angelo and N. Rynn. Diffusion of a Cold Cesium Plasma across a Magnetic Field, *Phys. Fluids,* vol. 4, no. 2, 275-276, 1961.
2. N.D'Angelo and N. Rynn. Low Frequency Oscillations in Cesium Thermionic Converters, *Phys. Fluids,* vol. 4, no. 8, 1054-1055, 1961.
3. N.D'Angelo and R.W. Motley. Low Frequency Oscillations in a Potassium Plasma, *Phys. Fluids*, vol. 6, no. 3, 422- 425, 1963.
4. F.F. Chen. "Universal" Overstability of a Resistive, Inhomogeneous Plasma, *Phys. Fluids*, vol. 8, no.7, 1323-1333, 1965.
5. H. W. Hendel, B. Coppi, F. Perkins and P.A. Politzer. Collisional Effects in Plasmas-Drift-Wave Experiments and Interpretation, *Phys. Rev. Lett.*, vol. 18, no. 12, 439-442, 1967.
6. E.Marden-Marshall, R.F.Ellis and J.E.Walsh. Collisional Drift Instability in a Variable Radial Electric Field, *Plasma Phys.,* vol. 28, no. 9B, 1461-1482, 1986.
7. J. Wesson, *Tokamaks*, 2nd ed. Oxford: Clarendon Press, 1997.
8. L. Spitzer, *Physics of Fully Ionized Gases*, 2nd ed. New York: John Wiley & Sons, 1967.
9. N.Krall and A. Trivelpiece, *Principles of Plasma Physics*, McGraw-Hill Kogakusha, LTD, 1973.
10. M. A. Lieberman and A. J. Lichtenberg, *Principles of Plasma Discharges and Materials Processing*, New Yprl: John Wiley & Sons, 1994.
11. Y. S. Satya and R. K.Kaw. Drift Waves in Turbulent Plasmas, *Phys. Rev. Lett.,* vol. 31, no. 24, 1453-1457, 1973.
12. A. J. Anastassiades, and C.L. Xaplanteris. Drift Wave Instability in the Presence of an RF-Field in a Magnetized Plasma, *J. Phys.Soc. of Jpn*, vol. 52**,** no. 2, 492-500, 1983.

13. C.L. Xaplanteris. Effect of Low-Frequency Instability on Hall Conductivity in Plasma, *Astrophys. Space Science,* vol. 139, no. 2, 233-242, 1987.
14. C.L. Xaplanteris. Collisional Instability in a Rare Magnetized Plasma: An Experimental Model for Magnetospheric and Space Plasma Study, *J. Plasma Physics*, vol. 75**,** no. 3, 395-406, 2009.
15. T. Klinger. *Handbook of Chaos Control*, ed. H. G. Schuster, (Wiley VCH, Weinheim, 513-562, 1998.
16. D. Block et al. Sychronization of Drift Waves, *Phys. Rev. E,* vol. 63**,** no. 5, 056401, 2001.
17. C. L. Xaplanteris and E. Filippaki. Drift Waves' Synchronization by Using an External Signal. The Stabilization of a Chaotic Plasma Turbulence, *Chaos Theory, Modeling Simulation and Applications*, eds. C. H. Skiadas, I. Dimotikalis, 2011.
18. C.L. Xaplanteris et al. Electron Drift Caused by rf Field Gradient Creates Many Plasma Phenomena: An Attempt to Distinguish the Cause and the Effect, *J. Plasma Physics*, vol. 78**,** no. 2, 165-174, 2012.